ASCE-ASME Journal of Risk and Uncertainty in Engineering Systems Part B: Mechanical Engineering. Received June 05, 2023;
Accepted manuscript posted February 19, 2024. doi:10.1115/1.4064766

Impact of sources of damping on the fragility estimates of wind turbine towers

Shubham Baisthakur[1], Vikram Pakrashi[2], Subhamoy Bhattacharya[3], and Breiffni Fitzgerald[1]

[1]School of Engineering, Trinity College Dublin, Dublin, Ireland. Email: breiffni.fitzgerald@tcd.ie
[2]UCD Centre for Mechanics, Dynamical Systems and Risk Laboratory, School of Mechanical and Materials Engineering, University College Dublin, Ireland.
[3]Department of Civil and Environmental Engineering, University of Surrey, UK.

ABSTRACT

Fragility estimates in wind turbine towers have been investigated but the the effect of damping on fragility has not been studied. While damping can often be small, it can come from different sources for a wind turbine. This paper demonstrates that even for small levels of equivalent viscous damping, a combination of sources can have a significant impact on the estimate of the fragility of a wind turbine in operational conditions. The widely studied 5MW reference wind turbine is considered for this study. The fragility analysis is performed considering the tower fore-aft displacement and acceleration responses. The impact of different sources of damping on fragility is estimated and ranked to qualitatively understand the impact of damping on the lifetime performance of the tower and develop approximate estimates of their quantitative changes.

INTRODUCTION

Wind turbines continue to grow in capacity and consequently in size [1, 2]. With this growth comes significant exposure to higher levels of lifetime wind loads [3]. Larger wind turbines are usually slender and flexible. Additionally, due to the increasing length of blades and towers in modern wind turbines, the fundamental frequencies of these structural components are low and usually below 0.5 Hz. This makes them dynamically wind sensitive and prone to wind-induced

ASCE-ASME Journal of Risk and Uncertainty in Engineering Systems Part B: Mechanical Engineering. Received June 01, 2023;
Accepted manuscript posted February 19, 2024. doi:10.1115/1.4064766

vibrations [4] and directly linked to their safety and serviceability limits. New materials are often being proposed for use in turbines [5] for better performance and commercial competitiveness, and control aspects are also being investigated in detail. Most of these studies focus on vibration control of the structural components for novel power control strategies [6–9], auxiliary damping devices [10–15] or structural modifications [16, 17].

On the other hand, existing wind turbines continue to degrade [18–20] and already generations of turbines and related wind farms are either coming to the end of their operational life [21] or have already been replaced [22]. Under such circumstances, remaining service life [23], degradation [24, 25] and assessment of effects of natural hazards on them [26–28] are becoming more important. Re-use of existing farms are being linked to geotechnical fatigue performance [29], while re-use of blades after their service life in a sustainable manner is also popular [22, 27, 30]. Whether it is a new structure, an evolving design or an existing set of wind turbines with the possibility of repair or control being installed, there is a need to compare them for relative assessment in terms of certain performance indicators for the choice of design, decision making or mitigation options. Since wind excitation is random and there are inherent uncertainties in turbine materials, models or geotechnical aspects, such a comparison is not trivial and is inadequately represented by single point comparisons, or even deterministic comparisons. Under such circumstances and probabilistic demands, the use of fragility curves have become popular for these types of comparisons [31, 32]. Fragility curves consider different limit states, variability of capacity and demand, and estimates probabilities of failures for such variabilities [33, 34]. It is thus also representative of the vulnerabilities of these structures and must be investigated in detail to understand what impacts lifetime safety and performance of wind turbines.

Consequently, it is of critical importance to understand the impact of parameters that can significantly affect the estimation of fragility curves, along with the impact of their variabilities. To do so, extensive numerical analyses are required, even to approach this understanding from a qualitative point of view. Observed variations in fragility estimates not only allow in understanding the importance of these parameters, but also the need for their monitoring, the accuracy with which

ASCE-ASME Journal of Risk and Uncertainty in Engineering Systems Part B: Mechanical Engineering. Received June 01, 2023;
Accepted manuscript posted February 19, 2024. doi:10.1115/1.4064766

they should be monitored and the consequences of uncertainties in their estimates on safety and performance of wind turbines over their operational life.

A key issue in this regard is damping. Damping is generally a difficult parameter to estimate [35–38] and can often lead to significantly different results in dynamic responses [39]. While there exists some work on fragility estimates around wind turbines [40, 41], there is no work, to the best of the knowledge of the authors investigating the impact of damping. There has been little work reported to date on the inherent sources of damping in a wind turbine and their different contributions to the dynamic response. Damping is notoriously difficult to quantify and model. The challenge is not trivial since there are multiple sources of damping in a wind turbine[42–44]. In addition to structural damping, there is also aerodynamic damping, soil damping, and, for offshore wind turbines, hydrodynamic damping, which contributes to the overall damping in the system. In practice, it is difficult to assess the individual contribution from each damping source to the dynamic response of the structure. This has led to large uncertainties in the design process. Consequently, the question is not only whether and how much the damping affects fragility curves but also which source of damping contributes in what way. This apportionment further relates to what damping sources should be considered, estimated or monitored more carefully. It also provides information on how scaled testing of such turbines can be carried out better [43, 45]. Furthermore, understanding these sources would also provide the basis for developing and modifying geotechnical and structural testing in the laboratory [46] and on-site.

Soil/foundation damping has been the least studied of all of the sources of damping in wind turbines and there exist large discrepancies between theoretical studies and field measurements [47]. It is generally assumed that the soil/foundation damping mechanism is hysteretic material damping [48]. In the field, this is usually quantified by the logarithmic decrement of the ambient vibration response of the turbine, however, more advanced output-only identification techniques have also been recommended in the literature [49]. A recent review of soil/foundation damping in wind turbines recommended that simple models be used in the early-stage design and that the foundation soil damping effects are heavily dependent on turbine geometry, ground conditions, and

ASCE-ASME Journal of Risk and Uncertainty in Engineering Systems Part B: Mechanical Engineering. Received June 01, 2023; Accepted manuscript posted February 19, 2024. doi:10.1115/1.4064766

loading effects [50].

Aerodynamic damping is another large source of damping in wind turbines. Similar to soil/foundation damping, it is difficult to characterise. Aerodynamic damping is a function of the aerodynamic design of the blades and their structural dynamic response to the aerodynamic load [51]. Aerodynamic damping can be either estimated numerically based on an aeroelastic model of the wind turbine or obtained from data measurement campaigns on operational wind turbines. Numerically, many schemes have been devised to obtain aerodynamic damping. Co-ordinate transformations have been used to estimate damping ratios from time-invariant matrices representing the wind turbine system [52], blade element momentum theory has also been used [53], and in recent studies, wavelet analysis has been used to estimate aerodynamic damping from aeroelastic simulations [54, 55]. In the field, it is difficult to quantify the aerodynamic damping due to its dependence on the aerodynamic loading. [56] and later [57] presented schemes for determining the aerodynamic damping from output-only system identification techniques applied to blade responses in experiments. These are the most widely regarded approaches in the literature however, they both require control or at least knowledge of the excitation, rendering them difficult to perform practically for an operational wind turbine.

Structural damping is a measure of energy dissipation in a vibrating structure and is another source of wind turbine damping. This is limited to the damping that is inherent in the structural materials and damping caused by relative motion between structural elements (e.g. at connections). This source of damping is relatively easier to estimate and model than soil/foundation damping and aerodynamic damping; however, it is still not straightforward. [58] studied the implications of the uncertainty of structural damping on a structure's response. The authors have stated that in the design of large flexible structures, structural damping is difficult to predict closer than plus or minus 30% until the structure is completed and direct measurements can be taken.

Irrespective of the variety of mechanisms through which damping sources manifest themselves, wind turbines in operational conditions are expected not to exhibit instability or extreme responses. For such situations, there are solutions related to design, control or operational shut-down to avoid

ASCE-ASME Journal of Risk and Uncertainty in Engineering Systems Part B: Mechanical Engineering. Received June 01, 2023;
Accepted manuscript posted February 19, 2024. doi:10.1115/1.4064766

these situations. However, it is the equivalent viscous damping representation of these sources, indicative of average energy loss over cycles, which still govern the responses of the turbine under standard operational aspects, typically in a linear regime. Even under such a standard situation, there can be significant variation in fragility estimates based on the sources of damping and minor variations in these small values. Despite this interesting and important possibility around lifetime performance, this has not been addressed or investigated.

This paper investigates how different sources of damping impact the fragility curves of wind turbines for different limit states. From the structural engineering perspective, the wind turbine tower is the single most important structural member, as the failure of the tower can lead to global failure. The impact of the damping properties of the structure on tower displacement is analysed. The safety and serviceability limit states of the wind turbine tower are expressed in terms of tower displacement and the probability of exceeding limit states is computed. A differential equation-driven model is chosen to model the wind turbine, which is representative of their behaviour in the reduced order [59] and a focus on the variability of fragility curves due to damping sources are investigated. The wind turbine tower and nacelle are the key areas of focus in this study since they often represent the more problematic aspects of wind turbine blades, which are easier to replace. The results not only provide the impacts of damping on design or assessment but is also useful in selecting materials, control aspects, soil-structure interaction considerations and monitoring strategies. The work can be transferred to other hazards like scour [60] and for offshore wind turbines [45, 61], where the older generation farms have already started to age. Finally, the results also have direct consequences for the assessment of other renewable energy devices (e.g. wave energy [62], floating solar [63]) and along the lines of the concept of modular energy islands [64].

The damping parameters investigated in this study are selected to represent the most commonly observed sources of damping in wind turbine operations. Following [65], who analysed the damped response of a wind turbine using a general frequency adaptive framework, a total of seven parameters are chosen to describe the damping properties of a wind turbine. This study develops a numerical model of a wind turbine following the Euler-Lagrange approach. The closed form equation for

ASCE-ASME Journal of Risk and Uncertainty in Engineering Systems Part B: Mechanical Engineering. Received June 01, 2023;
Accepted manuscript posted February 19, 2024. doi:10.1115/1.4064766

Mass, Stiffness and Damping matrices of the system are derived. The equation of motion is solved using the state-space method to obtain the wind turbine response under the action of aerodynamic loads under different damping conditions.

This study can thus rank the relative importance of commonly observed damping sources in a wind turbine through a fragility approach. The impact of each damping parameter under the action of aerodynamic loads is investigated. Further, the damping parameters are grouped at the member level, and the impact of member level damping is analyzed through the fragility approach. Since damping is a complex phenomenon, and it is difficult to capture all myriad mechanisms involved in energy dissipation, the equivalent viscous damping approach is considered and modelled as random variables in this study to also address uncertainty in damping estimation. The results can provide insight into the effect of damping on lifetime performance, further influencing design, monitoring and control aspects.

NUMERICAL MODEL OF WIND TURBINE

Wind turbines are designed to harness the kinetic energy of wind and convert it into electricity. The Rotor Nacelle Assembly (RNA), which consists of blades, shaft, gearbox, and generator, along with auxiliary mechanical and electronic components, is responsible for power production. The RNA is supported on the top of a wind turbine tower, which serves to achieve higher heights to access higher wind speeds and support the system loads with adequate reliability. In this study, a numerical model of the wind turbine system is developed with a major emphasis on accurately modeling the damping present in the system while simultaneously representing a realistic system response when subjected to random inflow conditions. The model assumes the wind turbine system to be linear elastic and the tower to be modelled using the principles of Euler-Brenoulli's beam, subjected to lumped mass and inertia at the top representing the RNA. The foundation flexibility is modelled using a spring and dashpot arrangement. The structure is assumed to be axially rigid and has only in-plane deformations. With these assumptions, the motion of the wind turbine model can be described entirely using four generalized coordinates, namely

ASCE-ASME Journal of Risk and Uncertainty in Engineering Systems Part B: Mechanical Engineering. Received June 01, 2023;
Accepted manuscript posted February 19, 2024. doi:10.1115/1.4064766

1. Rotation at the base/foundation ($q_{\theta,b}$)
2. Translation at the base/foundation ($q_{x,b}$)
3. Rotation at the tower top ($q_{\theta,t}$)
4. Translation at the tower top ($q_{x,t}$)

Here, the tower top translation ($q_{x,t}$) and rotation ($q_{\theta,t}$) are defined as the relative movement of the tower top after considering the effect of flexible foundation such that, under a finite rigid body displacement at the foundation ($q_{\theta,b} = \delta\theta, q_{x,b} = \delta x$), the tower top displacements are $q_{x,t} = 0$ and $q_{\theta,t} = 0$. These generalized coordinates are independent, completely describe the system at all times and make the system holonomic. Therefore, the Euler-Lagrange approach can be implemented to derive the equations of motion for this system. The tower is assumed to have uniform geometric and material properties with a constant flexural rigidity EI, a mass density μ, and a mass per unit length m_T. The RNA is modelled using a lumped mass M and lumped rotary inertia J at the tower top to consider the effect of inertia and rotation of blades. The effect of foundation flexibility is modelled using linear springs with stiffness parameters k_l, k_r, and k_{lr}, where k_l represent the resistance to lateral translation and k_r is the measure of resistance to rotation. The term k_{lr} models the coupling between translation and rotation at the foundation level. The damping in the system is contributed by the foundation, tower, and RNA. Damping offered by the soil at the foundation level is modelled using three damping parameters corresponding to damping in translation c_l, rotation c_r, and a coupling term c_{lr}. The damping parameters at the foundation level are assumed to follow viscous damping behavior. Structural damping in the tower is modelled as strain-rate dependent viscous damping c_1 and velocity-dependent viscous damping c_2. Aerodynamic damping is modelled using the parameters c_M and c_J, such that c_M is the measure of damping under linear motion at hub level and c_J represents the damping under rotational motion. These damping parameters are normalized with respect to the system properties and are modelled using corresponding non-dimensional parameters such that they can be used to study the behaviour of any general wind turbine model. The damping parameter and the suggested range of values by [65] for each parameter are presented in Table 1. The detailed derivation of the equation of motion

ASCE-ASME Journal of Risk and Uncertainty in Engineering Systems Part B: Mechanical Engineering. Received June 01, 2023;
Accepted manuscript posted February 19, 2024. doi:10.1115/1.4064766

is presented in the next section.

Derivation of Equations of Motion

The equations of motion are a fundamental tool for modelling and analyzing the dynamic behavior of wind turbines. In this section, we present the detailed derivation of the equations of motion for a representative wind turbine model. The schematic details of the numerical model are elaborated in Fig. 1. The model is based on an Euler-Bernoulli beam with a flexible base and subjected to a concentrated point load and moment at the free end. The equation for lateral displacement of the tower is derived using mode shape equations accounting for the flexibility of the foundation. The total potential and kinetic energy of the system is then derived which is used in the Lagrangian formulation to obtain the equilibrium equations for the four generalized coordinates. These equations describe the dynamic behavior of the wind turbine and are essential for modelling and analyzing its response to external loads. The list of symbols used to describe the structural properties of the model is included in Appendix I.

The tower is modelled as a cantilever beam, and the exact equation for lateral displacement of the tower with a flexible base and subjected to a concentrated point load and moment at the free end can be expressed as:

$$w(x,t) = q_{x,b}(t) + xq_{\theta,b}(t) + \frac{x^2}{2L^3}(3L - x)q_{x,t}(t) + \frac{x^2}{2L}q_{\theta,t}(t) \tag{1}$$

where x is the distance of a point on the tower from the tower base, such that $x = 0$ at the foundation level and $x = L$ at the free end where L is the height of the tower. The term $\frac{x^2}{2L^3}(3L - x)$ is the expression for the deformed shape of a cantilever subjected to a point load at its end, while the term $\frac{x^2}{2L}$ represent the deformed shape of the tower when subjected to a concentrated moment at its end. The effect of axial shortening of the tower due to lateral displacement is not considered. By removing the explicit time dependence for the convenience of representation, Eq.(1) can be represented as

$$w(x,t) = q_{x,b} + xq_{\theta,b} + \frac{x^2}{2L^3}(3L - x)q_{x,t} + \frac{x^2}{2L}q_{\theta,t} \tag{2}$$

ASCE-ASME Journal of Risk and Uncertainty in Engineering Systems Part B: Mechanical Engineering. Received June 01, 2023;
Accepted manuscript posted February 19, 2024. doi:10.1115/1.4064766

The potential energy (PE) of a system is the energy stored in the system due to its deformation and rotations. For the wind turbine model, the total potential energy (PE) of this system can be expressed in terms of strain energy due to foundation deformation and work potential of the tower as:

$$V = \frac{1}{2}k_l q_{x,b}^2 + \frac{1}{2}k_r q_{\theta,b}^2 + 2k_{lr} q_{x,b} q_{\theta,b} + \int_0^L \frac{1}{2} EI(x) \left(\frac{\partial^2 w(x,t)}{\partial x^2}\right)^2 dx \tag{3}$$

Substituting the Eq.(2) in Eq.(3) and solving the integral gives the final expression for potential energy as

$$V = \frac{1}{2}k_l q_{x,b}^2 + \frac{1}{2}k_r q_{\theta,b}^2 + 2k_{lr} q_{x,b} q_{\theta,b} + \frac{3EI}{2L^3} q_{x,t}^2 + \frac{EI}{2L} q_{\theta,t}^2 + \frac{3EI}{2L^2} q_{x,t} q_{\theta,t} \tag{4}$$

Similarly, the kinetic energy (KE) of the system can be calculated considering the inertial and rotational kinetic energy as:

$$T = \frac{1}{2}\int_0^L \mu(x) \left(\frac{\partial w(x,t)}{\partial t}\right)^2 dx + \frac{1}{2}M \left(\frac{\partial w(x,t)}{\partial t}\right)^2 + \frac{1}{2}J \left(\frac{\partial^2 w(x,t)}{\partial t \partial x}\right)^2 \tag{5}$$

Substituting the definition of $w(x,t)$ from Eq.(2) in Eq.(5), and integrating along the tower height gives the final expression for kinetic energy as:

$$\begin{aligned} T = &\left(\frac{m_T L + M}{2}\right) \dot{q}_{x,b}^2 + \left(\frac{ML^2}{2} + \frac{m_T L^3}{6} + \frac{J}{2}\right) \dot{q}_{\theta,b}^2 + \left(\frac{M}{2} + \frac{57 m_T L}{56} + \frac{9J}{8L^2}\right) \dot{q}_{x,t}^2 + \\ &\left(\frac{ML^2}{8} + \frac{m_T L^3}{20} + \frac{J}{2}\right) \dot{q}_{\theta,t}^2 + \left(ML + \frac{m_T L^2}{2}\right) \dot{q}_{x,b}\dot{q}_{\theta,b} + \left(M + \frac{3 m_T L}{8}\right) \dot{q}_{x,b}\dot{q}_{x,t} + \left(\frac{ML}{2} + \frac{m_T L^2}{6}\right) \dot{q}_{x,b}\dot{q}_{\theta,t} + \\ &\left(ML + \frac{11 m_T L^2}{40} + \frac{3J}{2L}\right) \dot{q}_{\theta,b}\dot{q}_{x,t} + \left(\frac{ML^2}{2} + \frac{m_T L^3}{8} + J\right) \dot{q}_{\theta,b}\dot{q}_{\theta,t} + \left(\frac{ML}{2} + \frac{13 m_T L^2}{120} + \frac{J}{2L}\right) \dot{q}_{x,t}\dot{q}_{\theta,t} \end{aligned} \tag{6}$$

Following the derived expressions of KE and PE, the equation of motion for this model can be obtained by applying the Euler-Lagrange equation for each generalized coordinate separately. The

ASCE-ASME Journal of Risk and Uncertainty in Engineering Systems Part B: Mechanical Engineering. Received June 01, 2023;
Accepted manuscript posted February 19, 2024. doi:10.1115/1.4064766

governing equation of Euler-Lagrange method is given as:

$$\frac{d}{dt}\left(\frac{\partial T}{\partial \dot{q}_i}\right) - \frac{\partial T}{\partial q_i} + \frac{\partial V}{\partial q_i} = Q_i \tag{7}$$

where T and V represent the KE and PE of the system, respectively, and Q_i refers to the generalized forces acting along the generalized coordinate q_i. In this study, corresponding the four generalized coordinates q_i, Q represents a force vector such that $Q = \{F_b, M_b, F_t, M_t\}$, where F_b and M_b are the force and moment acting at the foundation level along the coordinate $q_{x,b}$ and $q_{\theta,b}$, respectively whereas F_t and M_t correspond to the force and moment acting at the tower top along the coordinates $q_{x,t}$ and $q_{\theta,t}$, respectively. For an offshore wind turbine, F_b and M_b represent the hydrodynamic force and moment acting at the tower base, while the terms F_t and M_t represent the aerodynamic force and moment acting on the rotor area. For an offshore wind turbine, the hydrodynamic forces can be calculated using Morison's equation [66]. A submerged body with volume V_T, reference area A_T when subjected to the fluid flow with velocity v_w and mass density ρ_w, the hydrodynamic force can be calculated as the sum of drag effect and inertia effect as presented in Eq.(8), where C_m and C_d represent the inertia coefficient and the drag coefficient for the submerged body which are determined from experimental data.

$$F_b = \rho_w C_m V_T \dot{v}_w + \frac{1}{2}\rho_w C_d A_T v_w |v_w| \tag{8}$$

The tower top loading mainly comes from aerodynamic forces. The aerodynamic forces at any aerodynamic section can be computed using Eq.(9) and Eq.(10), where F_l represents the Lift force which acts perpendicular to the direction of the resultant wind velocity and F_d represents the Drag force which acts along the direction of the resultant wind.

$$F_l = \frac{1}{2}\rho V_r^2 C_l \tag{9}$$

$$F_d = \frac{1}{2}\rho V_r^2 C_d \tag{10}$$

ASCE-ASME Journal of Risk and Uncertainty in Engineering Systems Part B: Mechanical Engineering. Received June 01, 2023;
Accepted manuscript posted February 19, 2024. doi:10.1115/1.4064766

here ρ is the mass density of the wind inflow and V_r is the resultant wind velocity. In these equations, C_l and C_d are the lift force coefficient and drag force coefficient, which are characteristic properties of an airfoil section and depend on Reynold's number and angle of attack. In this study, we have used the blade element momentum (BEM) theory to calculate the angle of attack at an airfoil for different wind inflow conditions. BEM theory is widely used in wind turbine design and analysis applications for calculating aerodynamic forces. BEM theory combines the blade element theory and momentum theory to account for rotor geometry characteristics and flow states to compute the angle of attack at an airfoil section for any inflow conditions and operating parameters of the wind turbine. This angle of attack is then used to compute lift and drag coefficients and, subsequently, the aerodynamic forces. BEM equations are solved iteratively to find the feasible operating conditions at a blade section such that the local flow geometries and momentum conservation are valid. Here, the BEM equations are solved using the methodology proposed by [67] for faster convergence. Since computing these forces is not the focus of the current investigation, BEM theory is not presented in detail. Interested readers can refer to [68] for an in-depth discussion on BEM theory for wind turbines. To this end, the external force vector Q represents a conservative system of forces. By substituting the equations for KE (Eq.(6)) and PE (Eq.(4)), in the governing equation of Euler-Lagrange method (Eq.(7)), the equations of motion for the numerical model are obtained as:

$$\begin{aligned}(m_T L + M)\,\ddot{q}_{x,b} + \left(\frac{m_T L^2}{2} + ML\right)\ddot{q}_{\theta,b} + \left(\frac{3m_T L}{8} + M\right)\ddot{q}_{x,t} + \left(\frac{ML}{2} + \frac{m_T L^2}{6}\right)\ddot{q}_{\theta,t} + (c_l + c_2 L)\dot{q}_{x,b} + \\ (c_{lr} + \frac{c_2 L^2}{2})\dot{q}_{\theta,b} + k_l q_{x,b} + 2k_{lr} q_{\theta,b} = F_b \quad (11)\end{aligned}$$

$$\begin{aligned}\left(\frac{m_T L^2}{2} + ML\right)\ddot{q}_{x,b} + \left(\frac{m_T L^3}{3} + ML^2 + J\right)\ddot{q}_{\theta,b} + \left(\frac{11 m_T L^2}{40} + ML + \frac{3J}{2L}\right)\ddot{q}_{x,t} + \\ \left(\frac{ML^2}{2} + \frac{m_T L^3}{8} + J\right)\ddot{q}_{\theta,t} + c_r \dot{q}_{\theta,b} + c_{lr}\dot{q}_{x,b} + k_r q_{\theta,b} + 2k_{lr} q_{x,b} = M_b \quad (12)\end{aligned}$$

ASCE-ASME Journal of Risk and Uncertainty in Engineering Systems Part B: Mechanical Engineering. Received June 01, 2023;
Accepted manuscript posted February 19, 2024. doi:10.1115/1.4064766

$$\left(\frac{3m_T L}{8} + M\right)\ddot{q}_{x,b} + \left(\frac{11 m_T L^2}{40} + ML + \frac{3J}{2L}\right)\ddot{q}_{\theta,b} + \left(\frac{57 m_T L}{28} + M + \frac{9J}{4L^2}\right)\ddot{q}_{x,t} + \left(\frac{ML}{2} + \frac{13 m_T L^2}{120} + \frac{J}{2L}\right)\ddot{q}_{\theta,t} + \left(\frac{3c_1 t_t}{4L} + \frac{3c_2 L}{8} + c_M\right)\dot{q}_{x,t} + \left(\frac{C_2 L^2}{6}\right)\dot{q}_{\theta,t} + \frac{3EI}{L^3}q_{x,t} + \frac{3EI}{2L^2}q_{\theta,t} = F_t \tag{13}$$

$$\left(\frac{ML}{2} + \frac{m_T L^2}{6}\right)\ddot{q}_{x,b} + \left(\frac{ML^2}{2} + \frac{m_T L^3}{8} + J\right)\ddot{q}_{\theta,b} + \left(\frac{ML}{2} + \frac{13 m_T L^2}{120} + \frac{J}{2L}\right)\ddot{q}_{x,t} + \left(\frac{ML^2}{4} + \frac{m_T L^3}{10} + J\right)\ddot{q}_{\theta,t} + \left(\frac{c_1 t_t}{2} + c_J\right)\dot{q}_{\theta,t} + \frac{3EI}{2L^2}q_{x,t} + \frac{EI}{L}q_{\theta,t} = M_t \tag{14}$$

In these equations, t_t stands for the thickness of the wind turbine tower. These equations can be expressed in matrix form as follows:

$$\begin{pmatrix} m_T L + M & \frac{m_T L^2}{2} + ML & \frac{3m_T L}{8} + M & \frac{ML}{2} + \frac{m_T L^2}{6} \\ \frac{m_T L^2}{2} + ML & \frac{m_T L^3}{3} + ML^2 + J & \frac{11 m_T L^2}{40} + ML + \frac{3J}{2L} & \frac{ML^2}{2} + \frac{m_T L^3}{8} + J \\ \frac{3m_T L}{8} + M & \frac{11 m_T L^2}{40} + ML + \frac{3J}{2L} & \frac{57 m_T L}{28} + M + \frac{9J}{4L^2} & \frac{ML}{2} + \frac{13 m_T L^2}{120} + \frac{J}{2L} \\ \frac{ML}{2} + \frac{m_T L^2}{6} & \frac{ML^2}{2} + \frac{m_T L^3}{8} + J & \frac{ML}{2} + \frac{13 m_T L^2}{120} + \frac{J}{2L} & \frac{ML^2}{4} + \frac{m_T L^3}{10} + J \end{pmatrix}\begin{pmatrix} \ddot{q}_{x,b} \\ \ddot{q}_{\theta,b} \\ \ddot{q}_{x,t} \\ \ddot{q}_{\theta,t} \end{pmatrix}$$
$$+ \begin{pmatrix} c_l + c_2 L & c_{lr} + \frac{c_2 L^2}{2} & 0 & 0 \\ c_{lr} & c_r & 0 & 0 \\ 0 & 0 & \frac{3c_1 t_t}{4L} + \frac{3c_2 L}{8} + c_M & \frac{c_2 L^2}{6} \\ 0 & 0 & 0 & \frac{c_1 t_t}{2} + c_J \end{pmatrix}\begin{pmatrix} \dot{q}_{x,b} \\ \dot{q}_{\theta,b} \\ \dot{q}_{x,t} \\ \dot{q}_{\theta,t} \end{pmatrix}$$
$$+ \begin{pmatrix} k_l & 2k_{lr} & 0 & 0 \\ 2k_{lr} & k_r & 0 & 0 \\ 0 & 0 & \frac{3EI}{L^3} & \frac{3EI}{2L^2} \\ 0 & 0 & \frac{3EI}{2L^2} & \frac{EI}{L} \end{pmatrix}\begin{pmatrix} q_{x,b} \\ q_{\theta,b} \\ q_{x,t} \\ q_{\theta,t} \end{pmatrix} = \begin{pmatrix} F_b \\ M_b \\ F_t \\ M_t \end{pmatrix} \tag{15}$$

ASCE-ASME Journal of Risk and Uncertainty in Engineering Systems Part B: Mechanical Engineering. Received June 01, 2023;
Accepted manuscript posted February 19, 2024. doi:10.1115/1.4064766

The matrix equation can be represented in a generalised form as

$$[M]\{\ddot{q}\} + [C]\{\dot{q}\} + [K]\{q\} = [Q(t)] \tag{16}$$

Here, the matrices $[M]$, $[C]$ and $[K]$ represent the mass, damping and stiffness properties of the structure and the force vector $Q(t)$ represents the external forces acting on the system, at any time t. This numerical model is used to compute the response of a wind turbine to external dynamic loading. Since most wind turbine towers are axisymmetric, this model can be used to compute the response in both fore-aft and side-side directions. The system matrices should be modified accordingly to represent the system configuration in the concerning direction. This model can be used to study both onshore and offshore wind turbines by selecting appropriate spring stiffness values and force vector. This study focuses on onshore wind turbines, which are not subjected to hydrodynamic forces, but the methodology presented here can be applied to study offshore wind turbines as well.

The damping matrix derived in this study represents a generalized damping form. The non-zero off-diagonal terms in the damping matrix represent the coupling between the generalized coordinates, commonly observed during operation. This damping matrix can not be cast as the conventional mass and stiffness proportional damping matrix; therefore, the governing equations can not be decoupled through modal analysis. Since the system matrices for the structure are time-independent, this system can be modelled as a Linear-Time-Invariant (LTI) system. In this study, these equations are solved using the state-space method. It is also important to note here that since the comparison between the contribution of different damping parameters is carried out for established design conditions and operations over a lifetime, instability from the form of damping (e.g. non-linearity related to it) is not relevant for this fragility comparison. Under such circumstances, the equivalent viscous damping coefficients are to be compared for a relative analysis within the fragility framework.

ASCE-ASME Journal of Risk and Uncertainty in Engineering Systems Part B: Mechanical Engineering. Received June 01, 2023;
Accepted manuscript posted February 19, 2024. doi:10.1115/1.4064766

NUMERICAL SIMULATIONS AND INTERPRETATION

This section presents the modelling of the NREL 5MW reference turbine using the system matrices presented in the previous section and the simulation strategy adopted to derive the fragility curves with reference to the uncertainty in the damping parameter values. The NREL 5MW wind turbine is widely used as a reference model due to its realistic design. The geometric and material properties of this wind turbine model are adopted from [69], and the relevant properties are provided in Table 2.

The NREL 5MW wind turbine has three blades, each 63 m long, with different airfoil shapes optimally placed along the blade span. The airfoil characteristics are taken into account while calculating the aerodynamic forces using BEM theory to represent the realistic loading conditions. To simulate aerodynamic loads, a number of mean wind speed values ranging from cut-in to rated wind speeds are sampled. Since the effect of the pitch controller is not considered in this study, the wind speed values above the rated wind speed are not considered while computing the response. Nevertheless, the aim of this study is to quantify the relative impact of different damping sources so these results will be applicable for the entire range of operating wind speeds. For the sampled mean wind speed values, turbulent wind speed realisations are generated using TurbSim [70]. TurbSim is a stochastic, full-field, turbulent-wind simulator which uses a statistical model to numerically simulate time series of wind speed vectors. The wind speed time histories are generated for a turbulence intensity of 10%. Due to the stochastic nature of turbulent wind conditions, the random effects in wind speed generations play a major role in the uncertainty of wind turbine response to turbulent loading. To ensure that the uncertainty arising from the unpredictable nature of inflow wind does not impact the ranking of damping parameters, a total of six random wind speed time histories for each mean wind speed value are considered to capture a range of possible wind speed scenarios. For the generated random wind time series, the aerodynamic forces are computed using the BEM theory. For computing the aerodynamic forces it is assumed that the rotor speed varies linearly between the cut-in and rated wind speed. A constant rotor speed corresponding to the mean wind speed is assumed while analysing the structure. The aerodynamic forces are computed with

ASCE-ASME Journal of Risk and Uncertainty in Engineering Systems Part B: Mechanical Engineering. Received June 01, 2023;
Accepted manuscript posted February 19, 2024. doi:10.1115/1.4064766

the time discretisation of 0.05 seconds. The governing equations of the system are solved using the ode45 method in Matlab, which is a six-stage, fifth-order, Runge-Kutta method [71, 72]. This method uses adaptive step size control such that it dynamically chooses the time steps based on the error estimation such that a balance between efficiency and accuracy is achieved. The aerodynamic forces acting on the system at a time step chosen by the ode45 algorithm are calculated using linear time interpolation of the force vector. The wind turbine response is evaluated for 600 seconds, of which the first 200 seconds are not considered in the analysis to remove the transient effects. The transience period of 200 seconds is a conservative estimate based on the system response corresponding to the lowest damping in the system. The response of the numerical model for a mean wind speed of 7 m/s at a turbulence intensity of 10% are shown in Fig. 2 to demonstrate the model's capability to estimate the dynamic response. In Fig. 2, all the damping parameter values are set to their respective mean values. The properties of the rotor are presented in Table 3. The aerodynamic forces computed using this approach represent the realistic loading acting on the wind turbine. The numerical model developed in this study intentionally excludes intricate controller dynamics and nuanced geometric details, aiming for a streamlined representation to isolate and assess the impact of damping. Consequently, direct quantitative comparisons with the more comprehensive 23-degree-of-freedom FAST model [73] are limited by the intentional simplifications introduced. Nevertheless, when comparing the tower top deformation for steady wind speeds in proximity to rated wind speeds, our simplified model exhibits good agreement with the more detailed FAST model, with a maximum error of 5%. This variance is attributable to the intentional simplifications introduced in our model, underscoring the trade-off between model complexity and the overarching research objective of studying the impact of generalized damping on wind turbine structural dynamics. These comparisons are presented in Table 4.

Overall, the numerical model developed in this study provides a good approximation of a wind turbine system's response to random inflow conditions while accurately modeling the damping present in the system. This model is subsequently used for studying the contribution of the damping sources on the fragility of the structure.

ASCE-ASME Journal of Risk and Uncertainty in Engineering Systems Part B: Mechanical Engineering. Received June 01, 2023;
Accepted manuscript posted February 19, 2024. doi:10.1115/1.4064766

Fragility analysis to rank importance of damping sources

The fragility analysis performed in this study provides insight into the relative importance of different damping sources on wind turbine tower response and can be used to inform design decisions and maintenance strategies. By quantifying the probability of exceeding limit states for different damping parameters, the fragility analysis can help identify critical damping sources and prioritize efforts to improve the reliability and performance of wind turbines. Overall, the fragility analysis is an important step towards developing a comprehensive understanding of wind turbine behavior and improving the sustainability and efficiency of wind energy systems. To study how damping affects wind turbine tower displacement, a large number of damping parameters are simulated considering the Gaussian uncertainty model for the damping parameters, with the parameter bounds governed by the values specified in Table 1. A 30% coefficient of variation is chosen to represent the uncertainty in the accurate estimation of damping values in operation. Further research is needed to better understand the nature of damping parameters and their uncertainty quantification, but the contribution effects are well represented by considering this wide envelope. The mean wind speed values (U_{mean}) are sampled from cut-in to rated wind speed, and turbulent wind fields are generated using TurbSim [70]. The wind turbine response is evaluated at the generated wind fields corresponding to the sampled damping values of each damping parameter. For the generated wind fields, the observed maximum tower top displacement at all the simulated damping parameters is recorded. In Fig. 3, the solid line represents the mean value of the maximum tower displacement (δ_{max}) for each random wind field under the influence of uncertainty introduced by the damping parameters, while the confidence bounds (represented by the shaded region around the solid line) is a measure of the variance observed in the maximum displacement due to the randomness introduced by simulated damping parameters. This analysis is performed for six different wind fields, while the results corresponding to only three seeds are presented for brevity. This Figure illustrates how variations in the damping parameter values impact the tower displacement response. Further, from Fig. 3 it is evident that the relative impact of the damping parameter is independent of the inflow wind, and a consistent ranking of damping parameters can be established based on the observations

ASCE-ASME Journal of Risk and Uncertainty in Engineering Systems Part B: Mechanical Engineering. Received June 01, 2023;
Accepted manuscript posted February 19, 2024. doi:10.1115/1.4064766

of this study. For the results presented in Fig. 3, the numerical model is subjected to a random external dynamic loading envelope represented by the seed value, such that each seed represents a unique stochastic forcing vector corresponding to each mean wind speed acting on the wind turbine. For each seed value, the uncertainty is introduced by randomly sampled damping values therefore, the uncertainty in the observed maximum tower displacement is a function of the randomness introduced through the damping parameters. In this context, the spread of observed maximum displacement is only due to the uncertainty in the damping parameter values. To quantify the effect of various damping parameters, the parameters are varied one at a time. When uncertainty in a particular damping parameter is simulated, the other parameters are set to their respective mean values. Each damping parameter has a distinct effect on the displacement response. The extent of variations observed in tower displacement response is a measure of its sensitivity to the corresponding damping parameter. The dispersion of the tower displacement response is higher for the strain-rate dependent damping in tower (c_1) as compared to the other sources.

To quantify the impact of uncertainty in damping estimation, fragility analysis is performed. For the fragility analysis, the uncertainty in damping parameters is modelled assuming a Gaussian distribution model. In the realm of fragility analysis, the variability introduced by the stochastic nature of inflow wind significantly surpasses the uncertainty arising from damping parameters in wind turbine performance. To prevent the intertwining of these uncertainties, the fragility analysis exclusively considers a singular random seed. This deliberate choice aims to isolate the influence of damping, ensuring that the impact of stochastic wind inflow does not contribute to the fragility estimates. Consequently, the presented fragility curves are inherently ad-hoc, serving the specific purpose of relative ranking for damping parameters. A fragility curve corresponding to each damping parameter is generated by recording the number of observations for which a particular limit state is exceeded for the number of simulated samples for the selected damping parameter. While generating fragility curve for a damping parameter, the other damping parameters are set to their respective mean values. Since only a limited number of samples can be simulated due to computational limitations, the entire variability over the operational wind speeds may not be

ASCE-ASME Journal of Risk and Uncertainty in Engineering Systems Part B: Mechanical Engineering. Received June 01, 2023;
Accepted manuscript posted February 19, 2024. doi:10.1115/1.4064766

effectively captured. In this context, a maximum likelihood method to fit the fragility curve to the observed values proposed by [74] is used in this study. Here, a log-normal cumulative function is used to describe the fragility function, such that:

$$p(f|ws = u) = \Phi\left(\frac{\ln(u/\theta)}{\beta}\right) \tag{17}$$

where, $p(f|ws = u)$ is a probability that the limit state will be exceeded for a mean wind speed u, and the terms θ and β are parameters of the fragility function. These parameters are optimised to find a best fit fragility curve which has the highest probability of having produced the observed probability of failure under limited number of samples.The optimisation process is represented in Eq.(18) which maximises the likelihood function assuming a binomial functional form to find the actual probability of failure, where m represents the total number of wind speeds considered while N and n corresponds to the simulated number of damping parameters and the number of times the limit state has exceeded, respectively.

$$\{\theta_{opt}, \beta_{opt}\} = \underset{\theta,\beta}{\operatorname{argmax}} \prod_{j=1}^{m} \binom{n_j}{N_j} \times \Phi\left(\frac{\ln(u_j/\theta)}{\beta}\right)^{n_j} \times \left[1 - \Phi\left(\frac{\ln(u_j/\theta)}{\beta}\right)^{(n_j - N_j)}\right] \tag{18}$$

The fragility curve for tower fore-aft displacement is presented in Fig. 4. In this Figure, the importance of the damping parameter can be assessed by the spread of the failure region or the slope of the fragility curve such that a higher slope corresponds to the lesser impact of the damping parameter. In this case, since the damping parameters are set to their mean values, the onset of failure should not be the criteria for ranking the damping parameters, as the damping contribution from other parameters leads to a reduction in the observed displacement. Using a similar approach, another set of fragility curves is generated such that when uncertainty in a particular is assumed, the other damping parameters are set to zero. These fragility curves are presented in Fig. 5. Here, it is evident that the onset of failure is the same for all the damping parameters. Both these figures show that at any chosen wind speed, the probability of exceeding the tower displacement limit state is minimum for the strain-rate dependent damping (c_1), followed by the linear aerodynamic

ASCE-ASME Journal of Risk and Uncertainty in Engineering Systems Part B: Mechanical Engineering. Received June 01, 2023;
Accepted manuscript posted February 19, 2024. doi:10.1115/1.4064766

damping (c_M), and the rotational aerodynamic damping (c_J), respectively. The fragility analysis reveals that the fragility curves for the foundation damping parameters for translation and rotation have a step-like fragility curve. This suggests that these damping parameters do not significantly alter the tower fore-aft displacement response under operating conditions. Although these factors do reduce the displacement response, their impact can not be observed with the chosen limit state value and loading conditions. Specifically, since the magnitude of foundation level displacement is much smaller than the tower top displacement, the overall tower displacement is mainly governed by the displacement at the tower top. This behavior is demonstrated by the comparison of the lateral displacement response observed at the foundation level and the tower top for the generalized coordinates $q_{x,b}$ and $q_{x,t}$, as shown in Fig. 6. The impact of foundation damping on the foundation response is demonstrated in Fig. 7 by comparing the response at the minimum and maximum damping values. Fig. 7 shows that lower displacement values are observed at higher damping levels; however, due to the small magnitude of displacement, their contribution is not reflected in the generated fragility curves.

Further, the damping contributed by the foundation, tower and RNA are grouped together by clubbing the damping parameters corresponding to these members. Following a similar methodology, in the presence of the uncertainty coming from stochastic inflow wind, the spread of maximum tower top displacement with respect to the selected parameter group is used as the criteria to rank the importance of member-level damping. These results are presented in Fig. 8. Further, the resulting fragility curves are presented in Fig. 9. Here, a representative limit state value is used for every unique stochastic inflow to generate the fragility curves. In reference to Fig. 8 and Fig. 9, it can be concluded that the damping contribution from the tower has the highest impact on the tower displacement response, followed by RNA Damping and foundation damping, respectively.

A similar analysis is performed to study the impact of damping on the tower top acceleration response. This analysis is of particular interest as the nacelle in wind turbines houses various acceleration-sensitive equipment, which could undergo damage if a certain acceleration threshold is exceeded. The result of the sensitivity of maximum tower acceleration (a_{max}) to various damping

ASCE-ASME Journal of Risk and Uncertainty in Engineering Systems Part B: Mechanical Engineering. Received June 01, 2023;
Accepted manuscript posted February 19, 2024. doi:10.1115/1.4064766

parameters for different stochastic wind fields is presented in Fig. 10. The damping parameters follow a similar ranking as observed for the tower displacement response. In addition, the foundation damping in the lateral direction is observed to have more influence on the acceleration response than it is observed in the displacement response. An another set of sensitivity analyses is performed by grouping the damping contributed by structural elements, and the corresponding results are presented in Figure 11. Since acceleration response does not have a linear trend with mean wind speed, the fragility curve based sensitivity analysis is not performed. In this context, mean wind speed can not be used as an intensity measure for fragility analysis of tower fore-aft acceleration.

These limit states have been selected such that the fragility curves can demonstrate the effect of damping characteristics on displacement and acceleration response. In this context, the exact value of the limit state will not impact the ranking of damping parameters considered in this study. The fragility curves generated in this study are valid as long as the assumptions about the structural properties and numerical model are valid. Nevertheless, these fragility curves demonstrate how the uncertainty in various damping parameters can impact the performance of a wind turbine. Overall, the fragility analysis provides valuable insight into the relative importance of different damping sources on wind turbine tower response and can be used to inform design decisions and maintenance strategies. However, it is important to note that the fragility analysis has some limitations, and further research is needed to better understand the nature of damping parameters and their uncertainty quantification. Nonetheless, the fragility analysis is an important step towards developing a comprehensive understanding of wind turbine behavior and improving the sustainability and efficiency of wind energy systems.

Conclusions

In conclusion, this study highlights the importance of characterizing the impact of damping properties on wind turbine tower response for the safety and operation of wind turbines. The 2D numerical wind turbine model developed in this study, along with the closed-form equations for mass, stiffness, and damping matrices, can be used for preliminary analysis of any wind turbine. The fragility analysis performed in this study provides valuable insight into the relative importance

ASCE-ASME Journal of Risk and Uncertainty in Engineering Systems Part B: Mechanical Engineering. Received June 01, 2023;
Accepted manuscript posted February 19, 2024. doi:10.1115/1.4064766

of different damping sources on wind turbine tower response and can be used to inform design decisions and maintenance strategies. The analysis shows that the damping at the foundation level does not considerably affect the nacelle displacement and acceleration response, while the strain-rate dependent damping (c_1) has the highest impact on the wind turbine response. This analysis suggests that it is possible to control the acceleration and displacement response of the structure by modifying damping characteristics of the structure through active or passive control and it will also depend on material properties. The aerodynamic damping in the nacelle also considerably impacts the wind turbine response. The foundation damping can play a significant role in idling wind turbines; however, this perspective is not addressed in this study.

The analysis also shows that the structural properties can impact the electronic limit state concerning various sensors and equipment operations. Wind turbine manufacturers and operators should take this into account while designing the electronic systems in a wind turbine. In summary, this study provides valuable insights into the impact of damping properties on wind turbine tower response and highlights the need for further research in this area. It is important to note that the fragility analysis has some limitations, and further research is needed to better understand the nature of damping parameters and their uncertainty quantification. Additionally, the effect of foundation flexibility on wind turbine response can be studied using the model developed in this study. Future directions in this regard can also include the understanding of complex damping models, effects of model uncertainties and the propagation of such errors in fragility curves, along with coupling effects. It is expected that this work will encourage several studies in the direction of using damping as an important parameter to consider and compare within the context of fragility curves over the operational lives of wind turbines, impacting choice of design, control, sensor placement strategies. assessment and repowering decisions.

Data Availability Statement

The data, models, and code that support the findings of this study are available from the corresponding author upon reasonable request.

ASCE-ASME Journal of Risk and Uncertainty in Engineering Systems Part B: Mechanical Engineering. Received June 01, 2023;
Accepted manuscript posted February 19, 2024. doi:10.1115/1.4064766

Acknowledgments

This work is supported by the Sustainable Energy Authority of Ireland (SEAI) (grant no. 19/RDD/511). Vikram Pakrashi and Breiffni Fitzgerald would also like to acknowledge the funding of SEAI TwinFarm RDD/604, Remotewind RDD/613 and Science Foundation Ireland project NexSys 21/SPP/3756.

ASCE-ASME Journal of Risk and Uncertainty in Engineering Systems Part B: Mechanical Engineering. Received June 01, 2023; Accepted manuscript posted February 19, 2024. doi:10.1115/1.4064766

APPENDIX I. NOTATION

The following symbols are used in this paper to describe the structural properties of numerical model:

E	=	Young's modulus of tower (N/m^2);
I	=	mass moment of inertia of tower (kgm^2);
J	=	rotational inertia of RNA (kgm^2);
L	=	height of tower (m);
M	=	mass of RNA (kg);
m_T	=	mass per unit length of tower (kg/m); and
t_t	=	thickness of tower (m).

ASCE-ASME Journal of Risk and Uncertainty in Engineering Systems Part B: Mechanical Engineering. Received June 01, 2023;
Accepted manuscript posted February 19, 2024. doi:10.1115/1.4064766

References

[1] A Madariaga, I Martínez de Alegría, JL Martín, P Eguía, and S Ceballos. "Current facts about offshore wind farms". In: *Renewable and Sustainable Energy Reviews* 16.5 (2012), pp. 3105–3116.

[2] Bruno Srbinovski, Andriy Temko, Paul Leahy, Vikram Pakrashi, and Emanuel Popovici. "Gaussian mixture models for site-specific wind turbine power curves". In: *Proceedings of the Institution of Mechanical Engineers, Part A: Journal of Power and Energy* 235.3 (2021), pp. 494–505.

[3] John D Holmes. *Wind loading of structures*. CRC press, 2007.

[4] Jesper Winther Larsen and Søren RK Nielsen. "Non-linear dynamics of wind turbine wings". In: *International Journal of Non-Linear Mechanics* 41.5 (2006), pp. 629–643.

[5] Kieran O'Leary, Vikram Pakrashi, and Denis Kelliher. "Optimization of composite material tower for offshore wind turbine structures". In: *Renewable Energy* 140 (2019), pp. 928–942.

[6] Ervin A Bossanyi. "Individual blade pitch control for load reduction". In: *Wind Energy: An International Journal for Progress and Applications in Wind Power Conversion Technology* 6.2 (2003), pp. 119–128.

[7] Hazim Namik and Karl Stol. "Individual blade pitch control of a spar-buoy floating wind turbine". In: *IEEE transactions on control systems technology* 22.1 (2013), pp. 214–223.

[8] Biswajit Basu, Andrea Staino, and Malabika Basu. "Role of flexible alternating current transmission systems devices in mitigating grid fault-induced vibration of wind turbines". In: *Wind energy* 17.7 (2014), pp. 1017–1033.

[9] Breiffni Fitzgerald, Andrea Staino, and Biswajit Basu. "Wavelet-based individual blade pitch control for vibration control of wind turbine blades". In: *Structural Control and Health Monitoring* 26.1 (2019), e2284.

ASCE-ASME Journal of Risk and Uncertainty in Engineering Systems Part B: Mechanical Engineering. Received June 01, 2023;
Accepted manuscript posted February 19, 2024. doi:10.1115/1.4064766

[10] Matthew A Lackner and Mario A Rotea. "Structural control of floating wind turbines". In: *Mechatronics* 21.4 (2011), pp. 704–719.

[11] Akwasi F Mensah and Leonardo Dueñas-Osorio. "Improved reliability of wind turbine towers with tuned liquid column dampers (TLCDs)". In: *Structural Safety* 47 (2014), pp. 78–86.

[12] Nicola Caterino. "Semi-active control of a wind turbine via magnetorheological dampers". In: *Journal of Sound and Vibration* 345 (2015), pp. 1–17.

[13] Tadhg Buckley, Phoebe Watson, Paul Cahill, Vesna Jaksic, and Vikram Pakrashi. "Mitigating the structural vibrations of wind turbines using tuned liquid column damper considering soil-structure interaction". In: *Renewable energy* 120 (2018), pp. 322–341.

[14] Breiffni Fitzgerald, James McAuliffe, Shubham Baisthakur, and Saptarshi Sarkar. "Enhancing the reliability of floating offshore wind turbine towers subjected to misaligned wind-wave loading using tuned mass damper inerters (TMDIs)". In: *Renewable Energy* (2023).

[15] Saptarshi Sarkar and Breiffni Fitzgerald. "Fluid inerter for optimal vibration control of floating offshore wind turbine towers". In: *Engineering Structures* 266 (2022), p. 114558.

[16] A Staino, B Basu, and Søren RK Nielsen. "Actuator control of edgewise vibrations in wind turbine blades". In: *Journal of Sound and Vibration* 331.6 (2012), pp. 1233–1256.

[17] Breiffni Fitzgerald and Biswajit Basu. "Vibration control of wind turbines: recent advances and emerging trends". In: *Int. J. Sustain. Mater. Struct. Syst* 4 (2020), pp. 347–372.

[18] Maria Martinez-Luengo and Mahmood Shafiee. "Guidelines and cost-benefit analysis of the structural health monitoring implementation in offshore wind turbine support structures". In: *Energies* 12.6 (2019), p. 1176.

[19] Masoud Asgarpour and John Dalsgaard Sørensen. "Bayesian based diagnostic model for condition based maintenance of offshore wind farms". In: *Energies* 11.2 (2018), p. 300.

ASCE-ASME Journal of Risk and Uncertainty in Engineering Systems Part B: Mechanical Engineering. Received June 01, 2023;
Accepted manuscript posted February 19, 2024. doi:10.1115/1.4064766

[20] Chia Chen Ciang, Jung-Ryul Lee, and Hyung-Joon Bang. “Structural health monitoring for a wind turbine system: a review of damage detection methods”. In: *Measurement science and technology* 19.12 (2008), p. 122001.

[21] Lisa Ziegler, Elena Gonzalez, Tim Rubert, Ursula Smolka, and Julio J Melero. “Lifetime extension of onshore wind turbines: A review covering Germany, Spain, Denmark, and the UK”. In: *Renewable and Sustainable Energy Reviews* 82 (2018), pp. 1261–1271.

[22] Eva Topham and David McMillan. “Sustainable decommissioning of an offshore wind farm”. In: *Renewable energy* 102 (2017), pp. 470–480.

[23] Pierre Tchakoua, René Wamkeue, Mohand Ouhrouche, Fouad Slaoui-Hasnaoui, Tommy Andy Tameghe, and Gabriel Ekemb. “Wind turbine condition monitoring: State-of-the-art review, new trends, and future challenges”. In: *Energies* 7.4 (2014), pp. 2595–2630.

[24] Robbie Herring, Kirsten Dyer, Ffion Martin, and Carwyn Ward. “The increasing importance of leading edge erosion and a review of existing protection solutions”. In: *Renewable and Sustainable Energy Reviews* 115 (2019), p. 109382.

[25] R Lacalle, S Cicero, JA Alvarez, R Cicero, and V Madrazo. “On the analysis of the causes of cracking in a wind tower”. In: *Engineering Failure Analysis* 18.7 (2011), pp. 1698–1710.

[26] Branko M Radičević, Milan S Savić, Søren Find Madsen, and Ion Badea. “Impact of wind turbine blade rotation on the lightning strike incidence–A theoretical and experimental study using a reduced-size model”. In: *Energy* 45.1 (2012), pp. 644–654.

[27] Ammar Alshannaq, David Scott, Lawrence Bank, Mehmet Bermek, and Russell Gentry. “Structural re-use of de-commissioned wind turbine blades in civil engineering applications”. In: *Proceedings, American Society for Composites 2019 Annual Meeting, Georgia Tech, USA*. 2019.

[28] Shubham Baisthakur and Breiffni Fitzgerald. “A study of wind-wave misalignment for the Irish coastline and its effect on the wind turbine response”. In: *Civil Engineering Research*

ASCE-ASME Journal of Risk and Uncertainty in Engineering Systems Part B: Mechanical Engineering. Received June 01, 2023;
Accepted manuscript posted February 19, 2024. doi:10.1115/1.4064766

in Ireland (CERI) And Irish Transportation Research Network (ITRN) Conference. 2022, p. 531.

[29] Susan Waldron, Joanne Smith, Kenny Taylor, Carol McGinnes, Nathan Roberts, and David McCallum. "Repowering onshore wind farms: A technical and environmental exploration of foundation reuse". In: *Carbon Landscape and Drainage Knowledge Exchange Network-led report, Construction Scotland Innovation Centre, Glasgow, Scotland, UK* (2018).

[30] Kieran Ruane, Zoe Zhang, Angela Nagle, An Huynh, Ammar Alshannaq, Asha McDonald, Paul Leahy, Marios Soutsos, Jennifer McKinley, Russell Gentry, et al. "Material and Structural Characterization of a Wind Turbine Blade for Use as a Bridge Girder". In: *Transportation Research Record* 2676.8 (2022), pp. 354–362.

[31] Aidan Quilligan, Alan O'Connor, and Vikram Pakrashi. "Fragility analysis of steel and concrete wind turbine towers". In: *Engineering structures* 36 (2012), pp. 270–282.

[32] Breiffni Fitzgerald, Saptarshi Sarkar, and Andrea Staino. "Improved reliability of wind turbine towers with active tuned mass dampers (ATMDs)". In: *Journal of Sound and Vibration* 419 (2018), pp. 103–122.

[33] Janko Slavič, Igor Simonovski, and Miha Boltežar. "Damping identification using a continuous wavelet transform: application to real data". In: *Journal of Sound and Vibration* 262.2 (2003), pp. 291–307.

[34] George Vathakkattil Joseph, Guangbo Hao, and Vikram Pakrashi. "Fragility analysis using vibration energy harvesters". In: *The European Physical Journal Special Topics* 228 (2019), pp. 1625–1633.

[35] Sondipon Adhikari and Jim Woodhouse. "Identification of damping: part 1, viscous damping". In: *Journal of Sound and vibration* 243.1 (2001), pp. 43–61.

[36] Sondipon Adhikari and Jim Woodhouse. "Identification of damping: part 2, non-viscous damping". In: *Journal of Sound and Vibration* 243.1 (2001), pp. 63–88.

ASCE-ASME Journal of Risk and Uncertainty in Engineering Systems Part B: Mechanical Engineering. Received June 01, 2023;
Accepted manuscript posted February 19, 2024. doi:10.1115/1.4064766

[37] Sondipon Adhikari. "Lancaster's method of damping identification revisited". In: *J. Vib. Acoust.* 124.4 (2002), pp. 617–627.

[38] Vesna Jaksic and Vikram Pakrashi. "Robust skewness-Kurtosis descriptor for damping calibration from frequency response". In: *Journal of Aerospace Engineering* 26.4 (2013), pp. 887–893.

[39] Vicenç Méndez, Werner Horsthemke, Pau Mestres, and Daniel Campos. "Instabilities of the harmonic oscillator with fluctuating damping". In: *Physical Review E* 84.4 (2011), p. 041137.

[40] Leonardo Dueñas-Osorio and Biswajit Basu. "Unavailability of wind turbines due to wind-induced accelerations". In: *Engineering Structures* 30.4 (2008), pp. 885–893.

[41] John D Sørensen and Henrik S Toft. "Probabilistic design of wind turbines". In: *Energies* 3.2 (2010), pp. 241–257.

[42] Subhamoy Bhattacharya, Domenico Lombardi, and David Muir Wood. "Similitude relationships for physical modelling of monopile-supported offshore wind turbines". In: *International Journal of Physical Modelling in Geotechnics* 11.2 (2011), pp. 58–68.

[43] Subhamoy Bhattacharya, Domenico Lombardi, Sadra Amani, Muhammad Aleem, Ganga Prakhya, Sondipon Adhikari, Abdullahi Aliyu, Nicholas Alexander, Ying Wang, Liang Cui, et al. "Physical modelling of offshore wind turbine foundations for TRL (technology readiness level) studies". In: *Journal of Marine Science and Engineering* 9.6 (2021), p. 589.

[44] S Bhattacharya and S Adhikari. "Experimental validation of soil–structure interaction of offshore wind turbines". In: *Soil Dynamics and Earthquake Engineering* 31.5-6 (2011), pp. 805–816.

[45] Vesna Jaksic, Richard O'Shea, Paul Cahill, J Murphy, DP Mandic, and V Pakrashi. "Dynamic response signatures of a scaled model platform for floating wind turbines in an ocean wave basin". In: *Philosophical Transactions of the Royal Society A: Mathematical, Physical and Engineering Sciences* 373.2035 (2015), p. 20140078.

ASCE-ASME Journal of Risk and Uncertainty in Engineering Systems Part B: Mechanical Engineering. Received June 01, 2023;
Accepted manuscript posted February 19, 2024. doi:10.1115/1.4064766

[46] Alessandro Casaburo, Giuseppe Petrone, Francesco Franco, and Sergio De Rosa. "A review of similitude methods for structural engineering". In: *Applied Mechanics Reviews* 71.3 (2019).

[47] Germanischer Lloyd Windenergie. "Overall damping for piled offshore support structures'". In: *Guideline for the Certification of Offshore Wind Turbines,(Edn.)* (2005).

[48] W Carswell, J Johansson, F Løvholt, SR Arwade, C Madshus, DJ DeGroot, and AT Myers. "Foundation damping and the dynamics of offshore wind turbine monopiles". In: *Renewable energy* 80 (2015), pp. 724–736.

[49] Christof Devriendt, Pieter Jan Jordaens, Gert De Sitter, and Patrick Guillaume. "Damping estimation of an offshore wind turbine on a monopile foundation". In: *IET Renewable Power Generation* 7.4 (2013), pp. 401–412.

[50] Abdollah Malekjafarian, Soroosh Jalilvand, Paul Doherty, and David Igoe. "Foundation damping for monopile supported offshore wind turbines: A review". In: *Marine Structures* 77 (2021), p. 102937.

[51] Flemming Rasmussen, J Thirstrup Petersen, and H Aagaard Madsen. "Dynamic stall and aerodynamic damping". In: (1999).

[52] MH Hansen. "Aeroelastic stability analysis of wind turbines using an eigenvalue approach". In: *Wind Energy: An International Journal for Progress and Applications in Wind Power Conversion Technology* 7.2 (2004), pp. 133–143.

[53] V Valamanesh and AT Myers. "Aerodynamic damping and seismic response of horizontal axis wind turbine towers". In: *Journal of Structural Engineering* 140.11 (2014), p. 04014090.

[54] Bei Chen, Zili Zhang, Xugang Hua, Biswajit Basu, and Søren RK Nielsen. "Identification of aerodynamic damping in wind turbines using time-frequency analysis". In: *Mechanical Systems and Signal Processing* 91 (2017), pp. 198–214.

ASCE-ASME Journal of Risk and Uncertainty in Engineering Systems Part B: Mechanical Engineering. Received June 01, 2023;
Accepted manuscript posted February 19, 2024. doi:10.1115/1.4064766

[55] Bei Chen, Biswajit Basu, Xugang Hua, Zhouquan Feng, Zili Zhang, Zhengqing Chen, and Søren RK Nielsen. “Online DWT algorithm for identification of aerodynamic damping in wind turbines”. In: *Mechanical Systems and Signal Processing* 152 (2021), p. 107437.

[56] K Thomsen, J Thirstrup Petersen, E Nim, S Øye, and B Petersen. “A method for determination of damping for edgewise blade vibrations”. In: *Wind Energy: An International Journal for Progress and Applications in Wind Power Conversion Technology* 3.4 (2000), pp. 233–246.

[57] Morten Hartvig Hansen, Kenneth Thomsen, Peter Fuglsang, and Torben Knudsen. “Two methods for estimating aeroelastic damping of operational wind turbine modes from experiments”. In: *Wind Energy: An International Journal for Progress and Applications in Wind Power Conversion Technology* 9.1-2 (2006), pp. 179–191.

[58] A Kareem and K Gurley. “Damping in structures: its evaluation and treatment of uncertainty”. In: *Journal of wind engineering and industrial aerodynamics* 59.2-3 (1996), pp. 131–157.

[59] Ramon Varghese, Vikram Pakrashi, and Subhamoy Bhattacharya. “A Compendium of Formulae for Natural Frequencies of Offshore Wind Turbine Structures”. In: *Energies* 15.8 (2022), p. 2967.

[60] Luke J Prendergast, Kenneth Gavin, and Paul Doherty. “An investigation into the effect of scour on the natural frequency of an offshore wind turbine”. In: *Ocean Engineering* 101 (2015), pp. 1–11.

[61] Aldert Otter, Jimmy Murphy, Vikram Pakrashi, Amy Robertson, and Cian Desmond. “A review of modelling techniques for floating offshore wind turbines”. In: *Wind Energy* 25.5 (2022), pp. 831–857.

[62] Pierre Benreguig, James Kelly, Vikram Pakrashi, and Jimmy Murphy. “Wave-to-wire model development and validation for two OWC type wave energy converters”. In: *Energies* 12.20 (2019), p. 3977.

ASCE-ASME Journal of Risk and Uncertainty in Engineering Systems Part B: Mechanical Engineering. Received June 01, 2023;
Accepted manuscript posted February 19, 2024. doi:10.1115/1.4064766

[63] Sara Oliveira-Pinto and Jasper Stokkermans. "Assessment of the potential of different floating solar technologies–Overview and analysis of different case studies". In: *Energy conversion and Management* 211 (2020), p. 112747.

[64] Carlos Rebelo and Lambis Baniotopoulos. "Modular energy islands for sustainability and resilience–cost action: CA20109 "MODENERLANDS"". In: *And Resilience* (2022), p. 30.

[65] S Adhikari and S Bhattacharya. "A general frequency adaptive framework for damped response analysis of wind turbines". In: *Soil Dynamics and Earthquake Engineering* 143 (2021), p. 106605.

[66] JR Morison, Joseph W Johnson, and Samuel A Schaaf. "The force exerted by surface waves on piles". In: *Journal of Petroleum Technology* 2.05 (1950), pp. 149–154.

[67] S Andrew Ning. "A simple solution method for the blade element momentum equations with guaranteed convergence". In: *Wind Energy* 17.9 (2014), pp. 1327–1345.

[68] Patrick J Moriarty and A Craig Hansen. *AeroDyn theory manual*. Tech. rep. National Renewable Energy Lab., Golden, CO (US), 2005.

[69] J. M. Jonkman, S. Butterfield, W Musial, and G. Scott. *Definition of a 5-MW Reference Wind Turbine for Offshore System Development*. National Renewable Energy Laboratory, Technical Report, NREL/TP-500-38060, Golden, Colorado, 2009.

[70] Bonnie J Jonkman. *TurbSim user's guide: Version 1.50*. Tech. rep. National Renewable Energy Lab.(NREL), Golden, CO (United States), 2009.

[71] The MathWorks Inc. *MATLAB version: 9.13.0 (R2022b)*. Natick, Massachusetts, United States, 2022. URL: https://www.mathworks.com.

[72] Lawrence F Shampine and Mark W Reichelt. "The Matlab ODE suite". In: *SIAM journal on scientific computing* 18.1 (1997), pp. 1–22.

ASCE-ASME Journal of Risk and Uncertainty in Engineering Systems Part B: Mechanical Engineering. Received June 01, 2023;
Accepted manuscript posted February 19, 2024. doi:10.1115/1.4064766

[73] Jason Jonkman. "The new modularization framework for the FAST wind turbine CAE tool". In: *51st AIAA aerospace sciences meeting including the new horizons forum and aerospace exposition*. 2013, p. 202.

[74] Jack W Baker. "Efficient analytical fragility function fitting using dynamic structural analysis". In: *Earthquake Spectra* 31.1 (2015), pp. 579–599.

ASCE-ASME Journal of Risk and Uncertainty in Engineering Systems Part B: Mechanical Engineering. Received June 01, 2023;
Accepted manuscript posted February 19, 2024. doi:10.1115/1.4064766

TABLE 1. Damping parameters and non-dimensional definition

Source of damping	Non-dimensional parameter	Formula	Suggested values
Lateral foundation damping	ξ_l	$\frac{c_l L}{\eta_l \sqrt{m_T EI}}$	$[10^{-1}, 10^{-2}]$
Rotational foundation damping	ξ_r	$\frac{c_r}{\eta_r L \sqrt{m_T EI}}$	$[10^{-2}, 10^{-3}]$
Cross foundation damping	ξ_{lr}	$\frac{c_{lr}}{\eta_{lr} \sqrt{m_T EI}}$	$[10^{-1}, 10^{-4}]$
Strain-rate damping	ξ_1	$\frac{c_1}{L^2 \sqrt{m_T EI}}$	$[10^{-3}, 10^{-5}]$
Velocity dependent damping	ξ_2	$\frac{c_2 L^2}{\sqrt{m_T EI}}$	$[10^{-2}, 10^{-3}]$
Aerodynamic mass damping	ξ_M	$\frac{c_M L}{\sqrt{m_T EI}}$	$[10^{-1}, 10^{-3}]$
Aerodynamic rotary damping	ξ_J	$\frac{c_J}{L \sqrt{m_T EI}}$	$[10^{-2}, 10^{-4}]$

ASCE-ASME Journal of Risk and Uncertainty in Engineering Systems Part B: Mechanical Engineering. Received June 01, 2023;
Accepted manuscript posted February 19, 2024. doi:10.1115/1.4064766

TABLE 2. Properties of the NREL 5MW model

Structural Properties	Numerical values
Tower height (L)	90m
Average tower diameter (D)	4.85m
Average tower thickness (t_t)	0.023m
Number of blades	3
Blade length	63m
Young's modulus (E)	2.1×10^{11} N/sqm
Mass density (ρ)	7800kg/cum
Lumped mass (M)	296,780kg
Tower deformation limit state	0.42m
Acceleration limit state	0.001g m/s^2

ASCE-ASME Journal of Risk and Uncertainty in Engineering Systems Part B: Mechanical Engineering. Received June 01, 2023;
Accepted manuscript posted February 19, 2024. doi:10.1115/1.4064766

TABLE 3. NREL 5MW Rotor Properties

Rotor properties	Numerical value
Cut-in wind speed	3m/s
Rated wind speed	11.4m/s
Cut-out wind speed	25m/s
Minimum rotor speed	6.9rpm
Rated rotor speed	12.1rpm

ASCE-ASME Journal of Risk and Uncertainty in Engineering Systems Part B: Mechanical Engineering. Received June 01, 2023;
Accepted manuscript posted February 19, 2024. doi:10.1115/1.4064766

TABLE 4. Tower Fore-Aft Displacement Comparison between the Numerical model and FAST

Wind Speed (m/s)	TFA Displacement Numerical Model (m)	TFA Displacement FAST (m)	Percentage Deviation
9	0.372	0.353	5.11%
10	0.437	0.418	4.34%
11	0.498	0.485	2.61%

ASCE-ASME Journal of Risk and Uncertainty in Engineering Systems Part B: Mechanical Engineering. Received June 01, 2023;
Accepted manuscript posted February 19, 2024. doi:10.1115/1.4064766

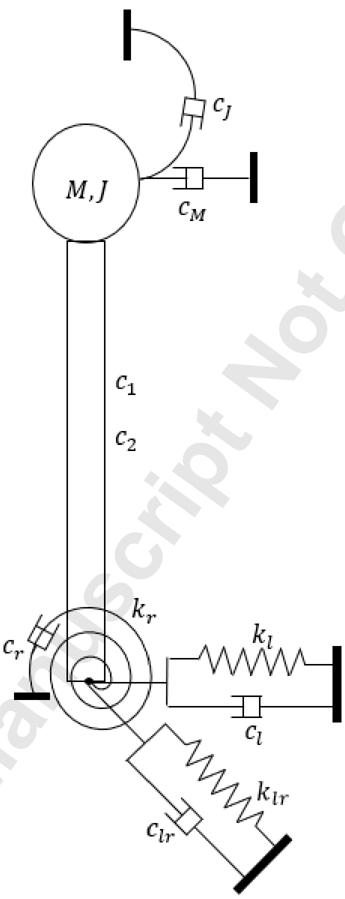

Fig. 1. Simplified mechanical model of a wind turbine

ASCE-ASME Journal of Risk and Uncertainty in Engineering Systems Part B: Mechanical Engineering. Received June 01, 2023;
Accepted manuscript posted February 19, 2024. doi:10.1115/1.4064766

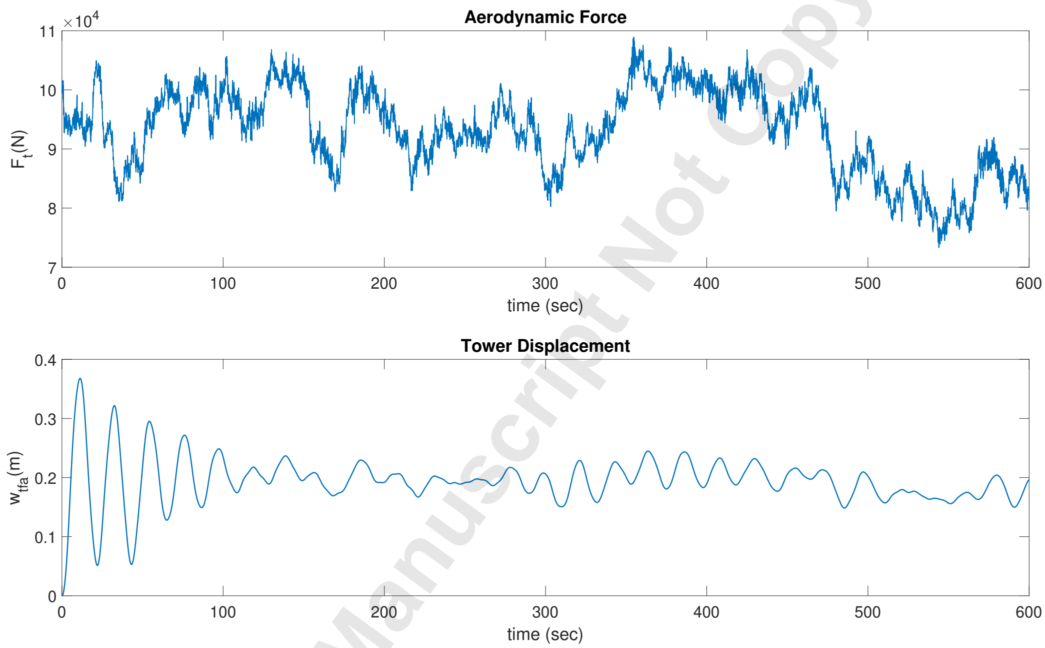

Fig. 2. Aerodynamic force and response of numerical model

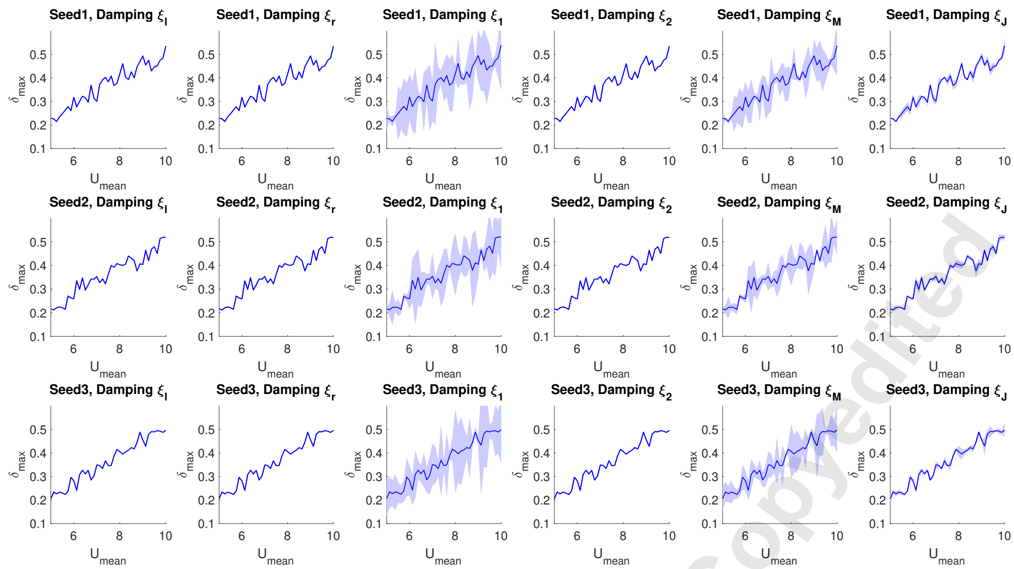

Fig. 3. Maximum tower displacement with confidence bounds representing the effect of uncertainty in damping parameters

ASCE-ASME Journal of Risk and Uncertainty in Engineering Systems Part B: Mechanical Engineering. Received June 01, 2023;
Accepted manuscript posted February 19, 2024. doi:10.1115/1.4064766

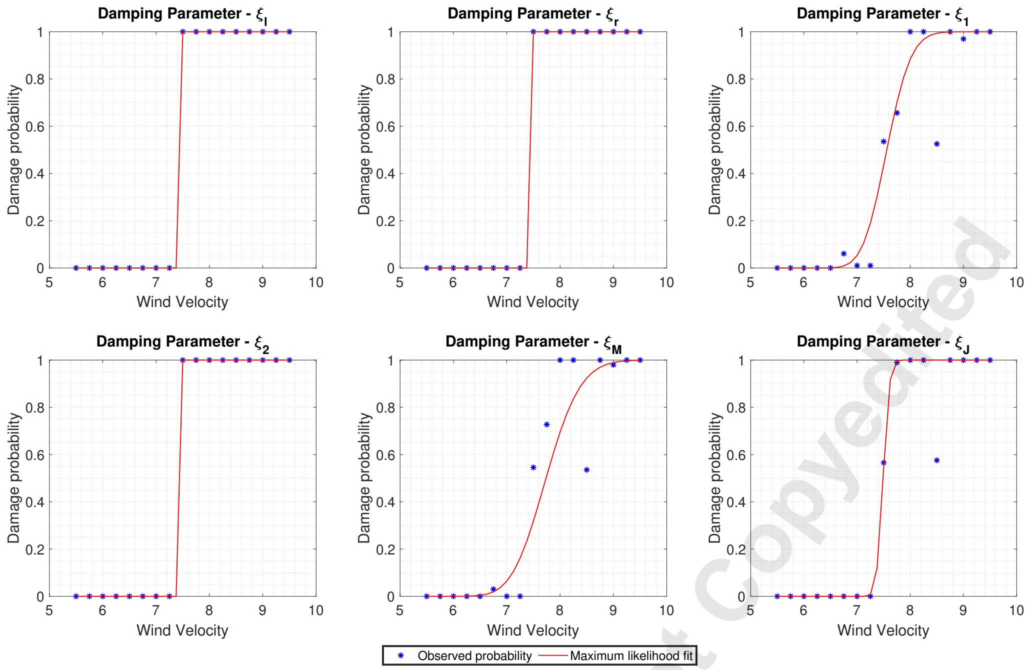

Fig. 4. Wind induced fragility curve for tower fore-aft displacement with mean damping as reference

ASCE-ASME Journal of Risk and Uncertainty in Engineering Systems Part B: Mechanical Engineering. Received June 01, 2023;
Accepted manuscript posted February 19, 2024. doi:10.1115/1.4064766

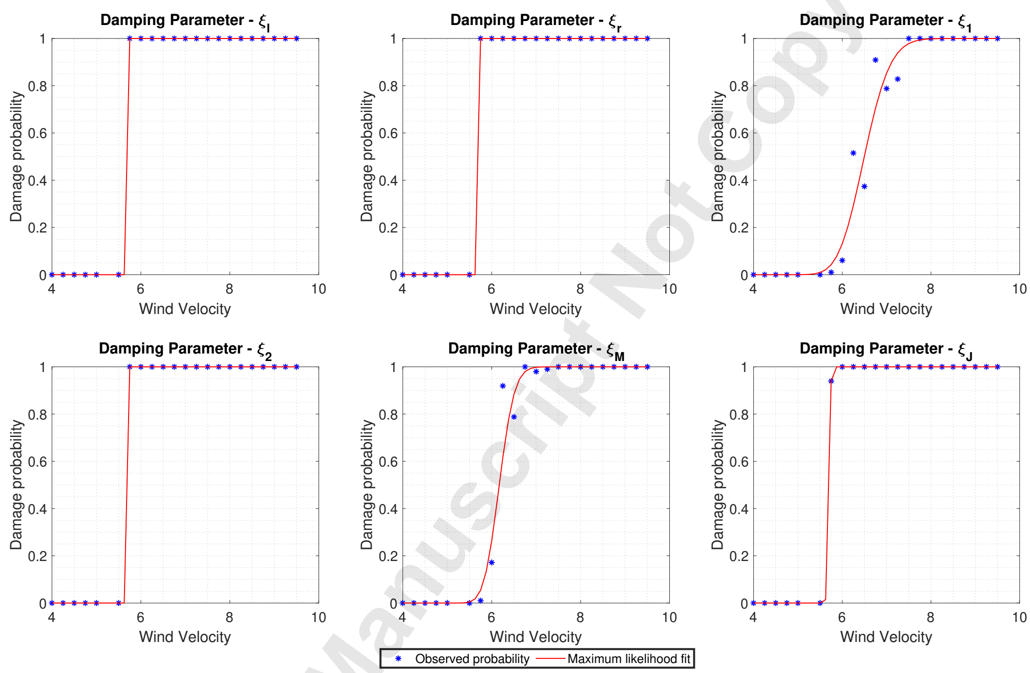

Fig. 5. Wind induced fragility curve for tower fore-aft displacement with undamped case as reference

ASCE-ASME Journal of Risk and Uncertainty in Engineering Systems Part B: Mechanical Engineering. Received June 01, 2023;
Accepted manuscript posted February 19, 2024. doi:10.1115/1.4064766

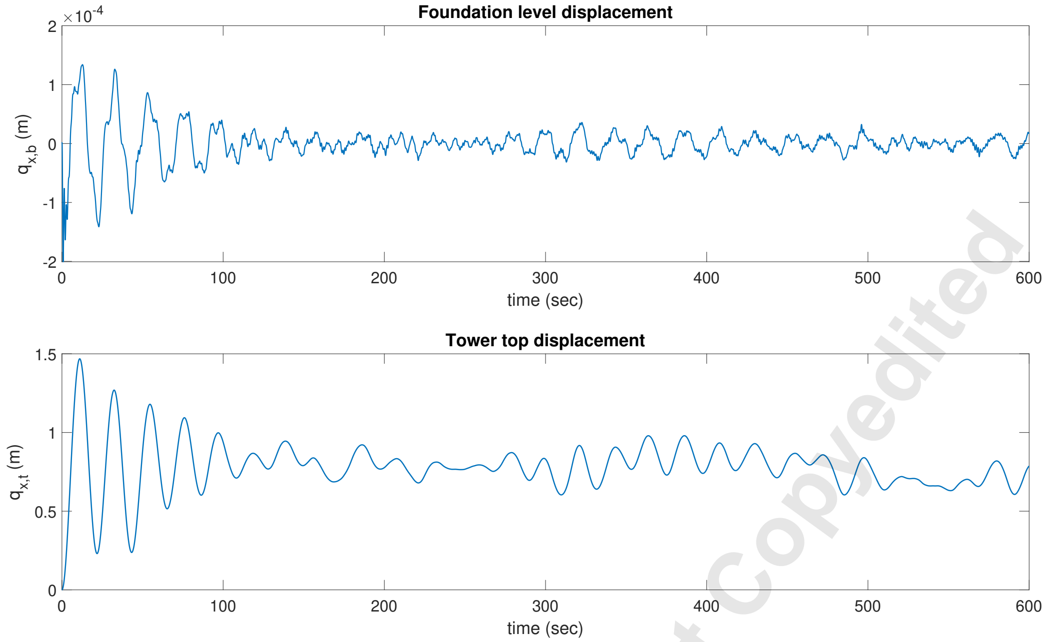

Fig. 6. Comparison of displacement at foundation level and tower top

ASCE-ASME Journal of Risk and Uncertainty in Engineering Systems Part B: Mechanical Engineering. Received June 01, 2023;
Accepted manuscript posted February 19, 2024. doi:10.1115/1.4064766

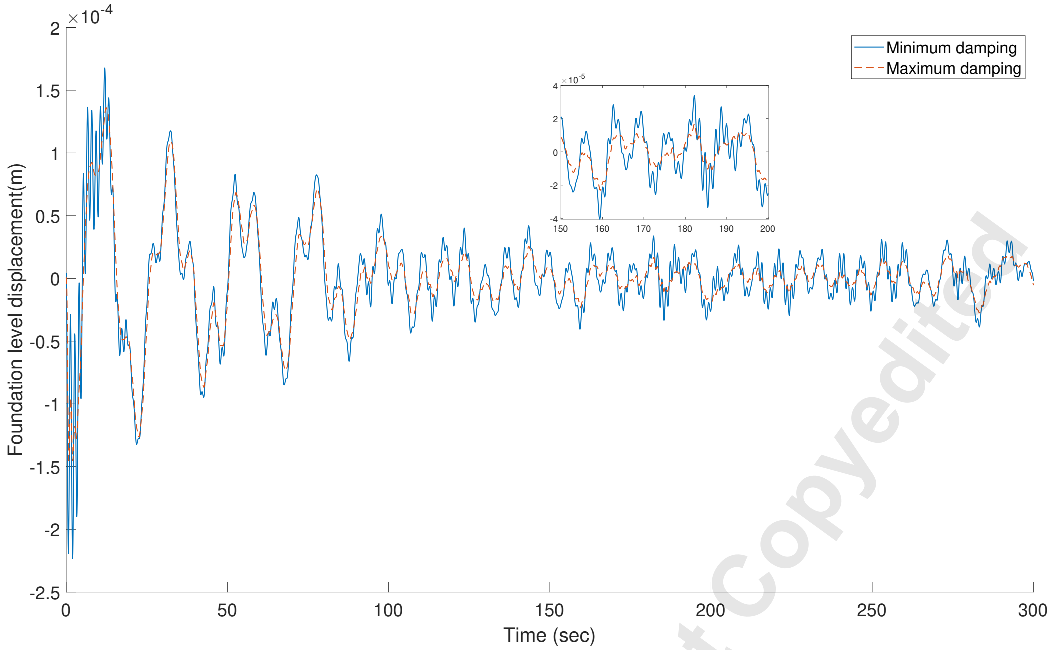

Fig. 7. Foundation displacement at minimum and maximum damping values

ASCE-ASME Journal of Risk and Uncertainty in Engineering Systems Part B: Mechanical Engineering. Received June 01, 2023;
Accepted manuscript posted February 19, 2024. doi:10.1115/1.4064766

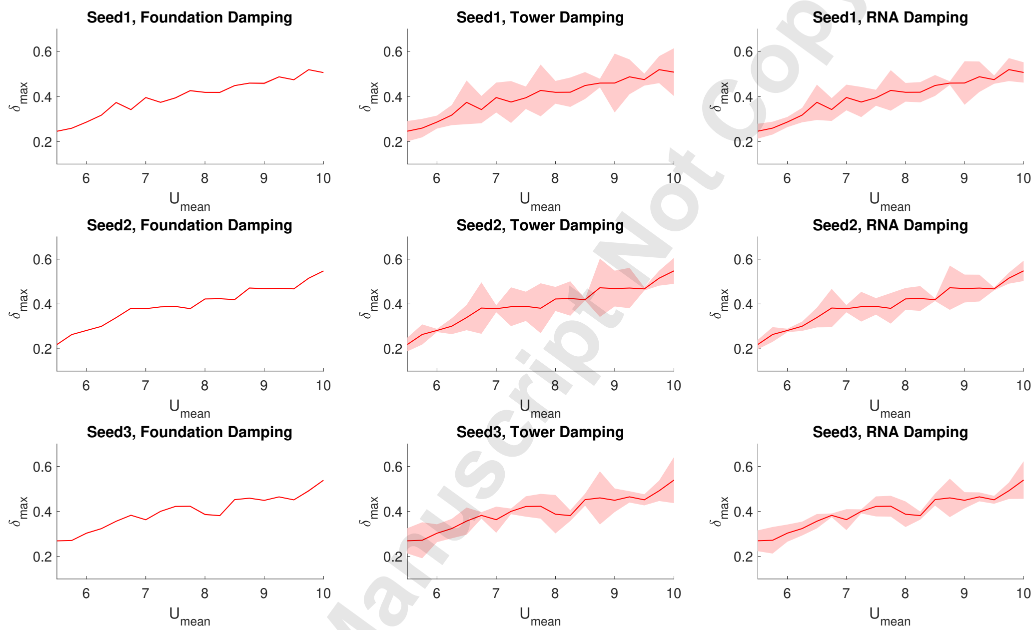

Fig. 8. Impact of uncertainty in member level damping on maximum tower displacement

ASCE-ASME Journal of Risk and Uncertainty in Engineering Systems Part B: Mechanical Engineering. Received June 01, 2023;
Accepted manuscript posted February 19, 2024. doi:10.1115/1.4064766

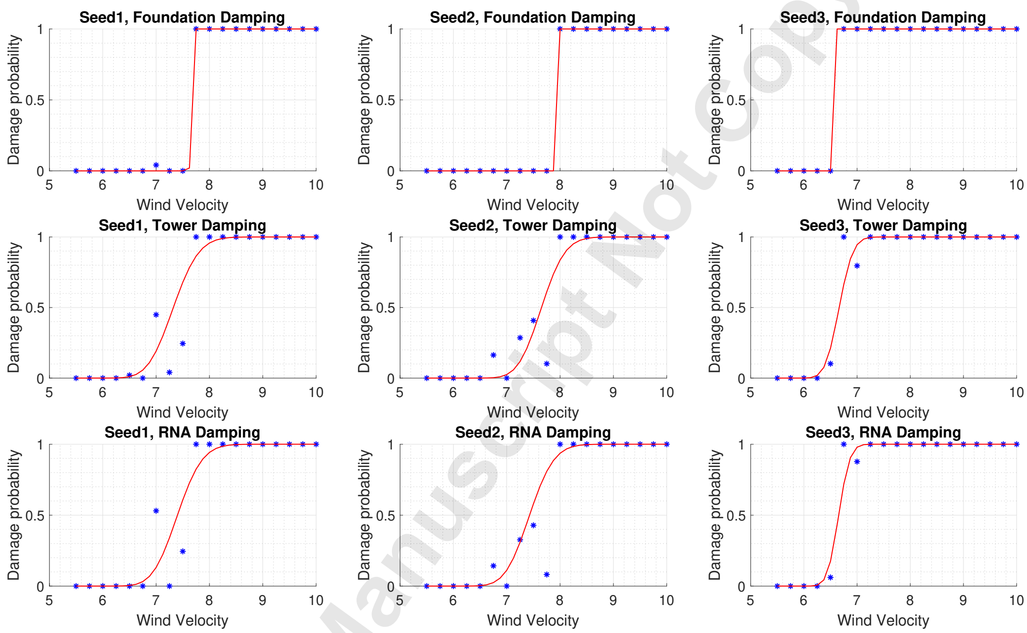

Fig. 9. Fragility curves for member level damping states

ASCE-ASME Journal of Risk and Uncertainty in Engineering Systems Part B: Mechanical Engineering. Received June 01, 2023;
Accepted manuscript posted February 19, 2024. doi:10.1115/1.4064766

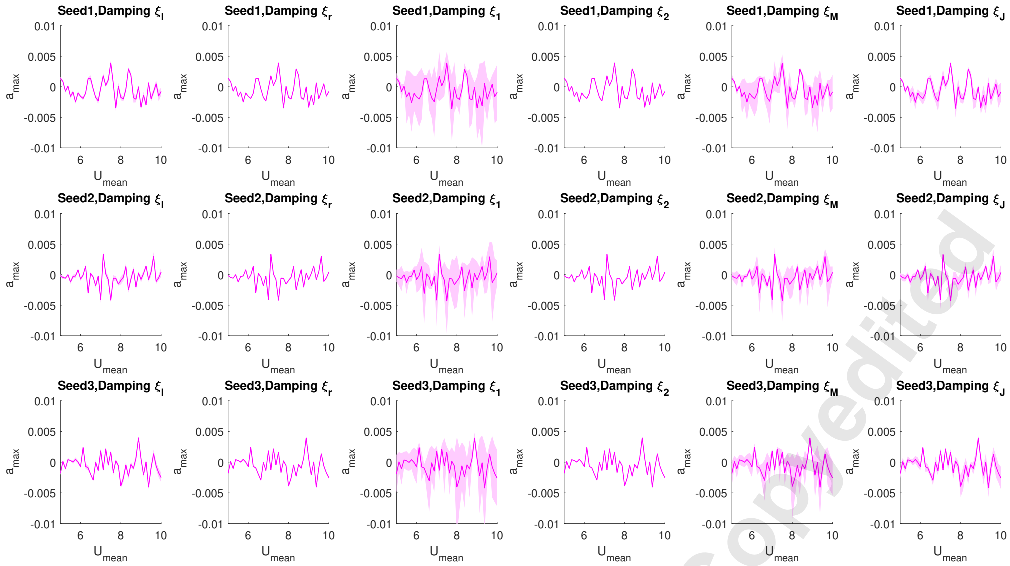

Fig. 10. Tower fore-aft acceleration with confidence bounds representing the effect of uncertainty in damping parameters

ASCE-ASME Journal of Risk and Uncertainty in Engineering Systems Part B: Mechanical Engineering. Received June 01, 2023;
Accepted manuscript posted February 19, 2024. doi:10.1115/1.4064766

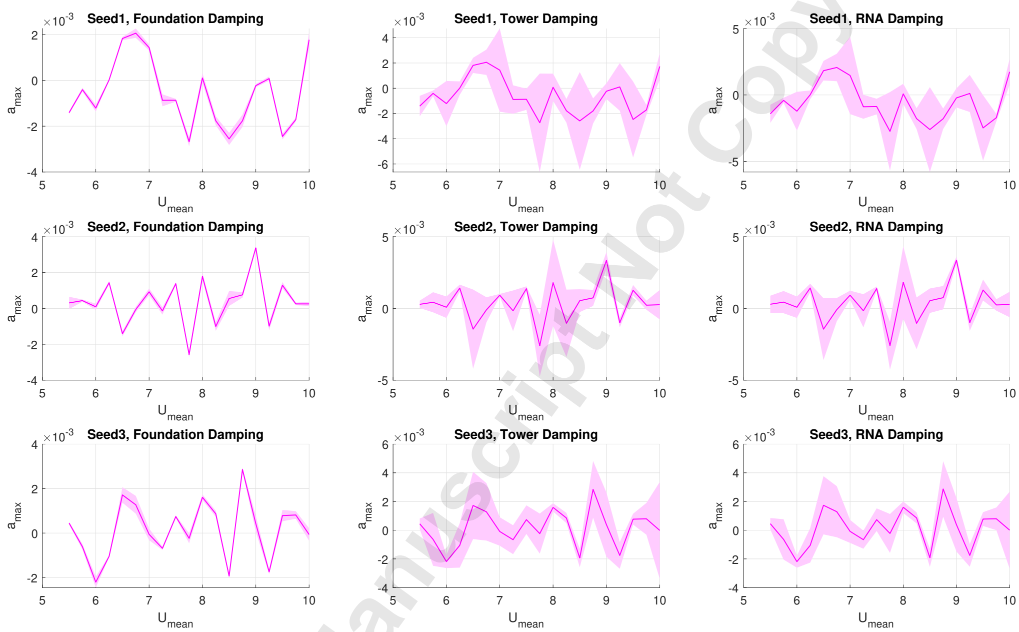

Fig. 11. Tower fore-aft acceleration with confidence bounds representing the effect of member level damping